Recent Stellar Occultation Observations Using High-Speed, Portable Camera Systems

A.A.S. Gulbis*, J.L. Elliot*†¶, M.J. Person*, B.A. Babcock‡, J.M. Pasachoff§, S.P. Souza§, and C.A. Zuluaga*

*Department of Earth, Atmospheric, and Planetary Sciences; †Department of Physics, Massachusetts Institute of Technology, Cambridge, MA 02139, USA
¶Lowell Observatory, Flagstaff, AZ 86001, USA
‡Physics Department; §Astronomy Department, Williams College, Williamstown, MA 01267, USA

Abstract. We have recently constructed six observing systems identified as POETS (Portable Occultation Eclipse and Transit System[1]). These systems are optimized for (i) high-speed, high signal-to-noise observations at visible wavelengths and (ii) easy transport, to allow mounting on telescopes worldwide. The Andor iXon cameras have e2v CCD97 (frame transfer) sensors: a 512 × 512 array of 16-micron pixels, back illuminated, with peak quantum efficiency > 90%. The maximum readout rate is 32 full frames per second, while binning and subframing can increase the cadence to a few hundred frames per second. Read noise in conventional modes goes below 6 electrons per pixel. Further, an electron-multiplying mode can effectively reduce the read noise to sub-electron levels, at the expense of dynamic range. The cameras are operated via a desktop computer that contains a 3 GHz Pentium 4 processor, 2 GB memory, and a 10,000 rpm hard disk. Images are triggered from a GPS receiver and have an approximately 50 nanosecond timing uncertainty. Each POETS can be transported as carry-on luggage. Here, we present instrument details, along with recent results from their use in stellar occultation observations by small bodies in the outer solar system. Occultations can produce data of the highest spatial resolution for any Earth-based observing method; therefore, they play a key role in determining diameters of distant solar-system bodies and probing the structure of atmospheres at the microbar level. We discuss POETS deployments in 2005-2007 to observe stellar occultations by Charon and Pluto (on 0.6- to 6.5-m telescopes) and future work on occultations by Kuiper Belt objects.

Keywords: optical instrumentation, solar system, occultation, eclipse, transit
PACS: 95.10.Gi, 95.55.Aq, 96.30.Sn, 96.30.Up, 96.30.Xa

INTRODUCTION

Since 2005, we have been deploying a set of high-speed, visible wavelength, portable camera systems called POETS (Portable Occultation Eclipse and Transit System) for observations of stellar occultations and similar events. Basic parameters of POETS are provided in the abstract above. Further details, including a block diagram of the system setup, are presented by Souza *et al*. [1]. Here, we present results from POETS observations of three stellar occultations by small bodies in the outer solar system. We provide additional characterization of POETS in the form of read noise and gain measurements for individual cameras as well as photometric observations. Finally, we discuss future plans for observing stellar occultations by Kuiper Belt objects (KBOs).

STELLAR OCCULATION OBSERVATIONS

To date, we have utilized POETS to observe three occultations by two small bodies in the outer solar system: Pluto and one of its moons, Charon. Our observations of each of these events have returned high-quality data from which we have been able to determine an accurate radius for Charon and probe the vertical structure of Pluto's atmosphere at different locations on the limb of the body.

We begin by providing a few practical notes on transporting and mounting the systems. A key aspect of POETS is that all components can be packed into two carry-on bags. These bags each weigh approximately 15 kg and fit into overhead luggage bins. All critical components are typically placed in one bag (camera, computer, GPS, and control cables). This allows the flexibility of checking the second bag and/or enables one person to transport a system alone. When the airplane is small enough to require carry-on luggage to be checked at the gate (such as flights between Santiago and La Serena, Chile, the headquarters site for Las Campanas Obs.), the camera alone has been hand carried. Airport security and customs have not presented significant issues, although people traveling with the system are routinely questioned about case contents and the electrical components are often checked for explosive residue.

For mounting purposes, we construct a plate that bolts to the camera faceplate and attaches just inside a telescope focal plane (configurations have included Cassegrain, Nasmyth, and Newtonian). Mounting options are diverse, as demonstrated by the setup at Mt. Stromlo for P384.2 (see below): the camera was attached to an optical table at the Coudé focus in a clean room. The camera–computer cable (6 m) is a limiting factor, and on larger telescopes we have often also mounted the computer and GPS to the telescope. While we prefer to have at least a few nights prior to the event to mount and test the systems, in practice we can operate on a significantly shorter timescale. An exemplary case was with the du Pont telescope for C313.2 (see below) in which unpacking the system, mounting to the telescope, a full night of observing, dismounting, and repacking were accomplished in a 24-hour period.

2005 July 11: C313.2 by Charon

Our first full test of POETS was in 2005, when we observed Charon occult the star C313.2.2 [2] (2UCAC 26257135; UCACMag = 14.8, where the UCAC bandpass is 579-642 nm [3]). We deployed our systems to four telescopes in South America: the Laboratório Nacional de Astrofísica's Observatório Pico dos Dias, Itajubá, Brazil (0.6 m); the Universidad Católica del Norte's Observatório Cerro Armazones, SE of Antofagasta, Chile (0.84 m); and Las Campanas Observatory's du Pont (2.5 m) and Clay (6.5 m) telescopes, near La Serena, Chile. All sites were successful except Pico Dos Dias, which was clouded out. The apparent occultation chord paths from each station are plotted in the top panel in Fig. 1a, along with a diagram of Charon at the time of the event. POETS data from the du Pont telescope is displayed in the bottom panel of Fig. 1a, to demonstrate the occultation light-curve shape for Charon.

This event was the first multichord observation of an occultation by Charon (the only other observation being a single chord obtained by Walker [4], 17 years earlier). POETS data, combined with an observation using the Acquisition Camera at the 8-m Gemini South, allowed us to determine the most accurate radius to date for Charon of

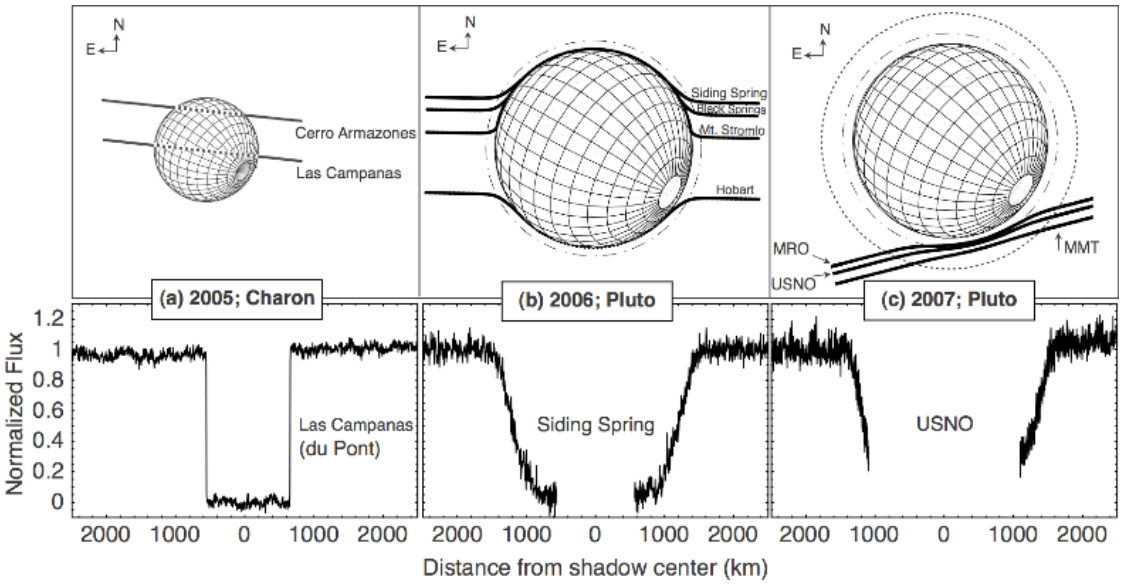

FIGURE 1. POETS data of the three stellar occultations discussed in this paper. *Top:* Occultation geometry for each event. Charon and Pluto's south poles (IAU convention) are on the right. Chords are shown for the 2005 event, while trajectories of the stellar image around Pluto's near limb are shown for the 2006 and 2007 events. These trajectories demark the location resulting from atmospheric refraction, where the star would have been observed if it were resolvable. For C313.2, the two Las Campanas chords are geographically close enough to be indistinguishable. The dot-dashed lines around Pluto represent the half-light shadow radii of 1207.9 ± 9.5 km [5] and 1207 ± 15 km [6], respectively. The dotted circle in the right-hand plot indicates a 2% drop in stellar flux. (figures following Gulbis *et al.* [7], Elliot *et al.* [5], and Person *et al.* [8]) *Bottom:* Normalized stellar flux from one POETS observation in the top panel is plotted as a function of distance from the shadow center – the break in the middle results from the chords not being central on the body. In 2005 the du Pont chord came within 11 km of shadow center and thus the break is not discernable in the plot. Relative velocities for these events were 21.33, 24.00, and 6.78 km/s. The varying shapes of these light curves illustrate the differences between the observations (full occultation versus graze) and between Pluto and Charon (in size and atmosphere).

606 ± 8 km [7] (this was later refined with others' data to be 606.0 ± 1.5 km [9]). At the Las Campanas Clay telescope, we obtained a light curve of particularly high signal-to-noise ratio (SNR; 273, over a 1-sec. cycle), which exhibited a diffraction fringe. Using these data, we verified that Charon has no substantial atmosphere and placed a 3σ upper limit on number densities of atmospheric candidate gases. A more complete description of the instrument setup, data, and analyses for this event can be found in Gulbis *et al.* [7], Person *et al.* [9], and Souza *et al.* [1].

2006 June 12: P384.2 by Pluto

In 2006, Pluto was predicted to occult the star P384.2 [2] (2UCAC 26039859, UCACMag = 15.0). Our collaboration deployed POETS to five sites in Australia and New Zealand: the Australian National University telescope at Siding Spring (2.3 m), the Star Castle Observatory at Black Springs (0.8 m), the Electro Optic Systems telescope at Mt. Stromlo (1.8 m), the Mt. Canopus Observatory near Hobart, Tasmania (1 m), and the McLellan telescope at Mt. John University Observatory, New Zealand (1 m). All sites for this event, except Mt. John (which was snowed out), successfully obtained data. The resulting stellar trajectories are shown in the top panel of Fig.1b. Our highest quality data for this event came from Siding Spring (SNR=96 over one pressure scale height of ~ 60 km), which are displayed in the bottom panel of Fig. 1b.

Data from the P384.2 event established that the overall structure of Pluto's atmosphere was relatively unchanged between 2002 and 2006. The upper atmosphere (≥1230 km radius) had temperature ~100 K, and the lower part of the atmosphere showed no evidence of the extinction and/or strong thermal gradient that were present in 1988. The 2006 also data provided an extended timeline for comparison with frost-migration models: by combining the 2006, 2002, and 1988 datasets, we predicted that Pluto will retain a substantial atmosphere through the 2015 flyby of NASA's *New Horizons* spacecraft. In addition, we used the 2006 data to constrain Pluto's surface radius. (See Elliot *et al.* [5] for complete analyses and discussion of this event.)

2007 March 18: P445.3 by Pluto

A particularly slow relative velocity prompted us to observe the 2007 predicted occultation by Pluto of the star P445.3 [2] (2UCAC 25823784, UCACMag = 15.3). For this event, POETS were transported to four stations in the Southwestern United States: the MMT Observatory in Arizona (MMTO; 6.5 m), the Large Binocular Telescope Observatory in Arizona (LBTO; 8.4 m), the Magdalena Ridge Observatory in New Mexico (MRO; 2.4 m), and the U.S. Naval Observatory Flagstaff Station in Arizona (USNO; 1.55 m). All sites successfully obtained data, although commissioning issues at LBTO resulted in the usage of a facility guide camera rather than POETS. The geometry of this event is shown in the top panel of Fig. 1c and demonstrates that the star grazed Pluto's upper atmosphere as seen from our stations. The grazing nature of this event is evident in the POETS light curve from the USNO presented in the lower panel of Fig. 1c. Although P445.3 is similar in brightness to P384.2 and C313.2, the SNR of these data (SNR=76 over one pressure scale height), suffered slightly because of the high air mass (~2 at event midtime).

The viewing geometry of this event, coupled with the slow velocity of P445.3, allowed for an unprecedented probe of Pluto's upper atmosphere. Exceptional-quality data were obtained at MMTO (SNR=336 over one pressure scale height), revealing large-scale, coherent wave structures in Pluto's atmosphere [6, 8, 10, 11]. At the time of writing, these results are not yet in press and we are exploring the relationship between the observed light curve structures and Pluto's atmospheric dynamics.

POETS CHARACTERIZATION

Read Noise and Gain

Stellar occultations provide opportunities to gain highly accurate information about objects in the solar system via ground-based observations (the spatial resolution is limited by diffraction, which is a few km at Pluto, for example). Achieving data with the greatest spatial resolution on the occulting body requires observations at high time resolution. High time resolution, and a suitable SNR, require the fastest cadence at which the photon noise is comfortably above the read noise. Therefore, the read noise of the instrument is a critical factor in our observation strategy.

Andor iXon cameras are the foundation of POETS. These cameras possess a variety of operational settings. There are two on-chip readout registers, conventional and electron multiplying (EM). In EM mode, a secondary gain register causes transferred electrons to undergo impact ionization, effectively strengthening the observed signal without increasing read noise. Note, however, that there is an amplification noise factor of up to $\sqrt{2}$ in EM mode due the statistical nature of the EM process. The output of either register is routed to a preamp stage with up to three possible gain settings. This signal is then fed to one of two Analog to Digital Converters (ADC): a 16-bit ADC with readout rate 1 MHz or a 14-bit ADC with readout rates 3, 5, or 10 MHz. Only the 1 and 3 MHz rates are available in conventional mode, while all rates function in EM mode. Each setting (and each camera) has slightly different characteristics. In Table 1, we present the measured read noise and gain for each of our functioning cameras. All values for the conventional modes are listed, as this regime was employed for the occultation observations presented here. Representative measurements are provided for EM modes for one camera. These values are particularly sensitive to EM setting and can vary widely from camera to camera.

Photometry

In order to determine the optimal bandpass for an occultation observation (or the effective wavelength of a past observation), the spectral response of the instrument, the spectrum of the light source, the transmission of the atmosphere (including airmass effects), and any wavelength dependence of the telescope optics must be considered. The light source, atmosphere, and telescope vary between our observations, but the POETS response depends only on the CCD and the filter. (The single iXon camera window is fused silica with a 400-900 nm broadband, anti-reflection coating and is not taken into consideration here.) In Fig. 2, we have plotted the camera response for a standard set of POETS filters. This set consists of filters 1.25” in diameter that slide

TABLE 1. Measured Characteristics of POETS Andor iXon Cameras.[a]

Conventional[b]				
Camera:	**Gain (e˜/ADU)**		**Read Noise (e˜)**	
preamp	*1MHz*[d]	*3MHz*	*1MHz*[d]	*3MHz*
X-3020: *1x*	3.70	9.78	8.58	13.56
2.4x	1.47	3.89	6.35	10.04
5x	0.66	1.78	5.83	9.49
X-2171: *1x*	4.19	11.02	9.18	15.18
2.4x	1.56	4.28	6.58	11.21
4.7x	0.67	1.83	5.88	9.83
X-2115: *1x*	3.98	10.73	9.81	14.84
2.4x	1.60	4.37	7.45	11.92
4.7x	0.73	2.00	6.69	10.34
X-1827: *1x*	3.66	8.87	8.29	14.55
2.4x	1.48	3.52	6.16	9.88
5.1x	0.68	1.67	5.65	8.80
X-1484: *1x*	3.99	9.29	8.17	15.53
2.4x	1.65	3.92	5.93	10.82
4.7x	0.87	2.06	5.64	10.10

Electron Multiplying (EM = 40)[c]			
X-3020 preamp	*1x*	*2.4x*	*4.7x*
Gain (e~/ADU*)*			
1 MHz[d]	0.29	0.12	0.06
3 MHz	0.69	0.28	0.13
5 MHz	0.70	0.29	0.13
10 MHz	0.74	0.31	0.14
Read Noise (e~)			
1 MHz[d]	0.56	0.36	0.30
3 MHz	0.78	0.47	0.40
5 MHz	1.05	0.66	0.19
10 MHz	1.10	0.70	0.48

[a] Values are the mean of multiple measurements.
[b] Cameras air cooled between –50º and –70º C.
[c] Camera was air cooled to –70º C. Tests at EM = 100 demonstrated an even further reduction in all values.
[d]

into a filter drawer, which has a T-mount interface to the camera and telescope. *B, V, R,* and *I* are composite Schott glass filters from Schüler, based on the Johnson-Cousins system. Schott glass filters have an advantage over coated filters because the spectral shape does not change with *f*-ratio; however, peak transmission is <90%. POETS' long-pass filters are from Baader Planetarium and are treated with coatings that allow very low scattered light and high (> 98%) peak efficiency.

To gauge the photometric capabilities of POETS, we utilized the 0.6-m telescopes at MIT's Wallace Astrophysical Observatory and the Hopkins Observatory of Williams College. At Wallace, we imaged bright standard stars to measure photometric accuracy. At Hopkins Observatory, we conducted observations to check the relative photometric accuracy near the practical faint limit set by sky conditions.

We performed bright standard star observations at Wallace on 2007 July 31, using POETS X-2171 with Schüler *V* and *R* filters. The seeing on this night was fair (~5 arcsec), as was the transparency. We employed the 1 MHz conventional mode with preamp gain of 2.4x, and exposure times ranged between 1 and 7 sec. The standard stars, listed in Table 2, were imaged over a range of airmasses from 1.07 to 1.53. Data were reduced with biases and sky flats, and aperture photometry was carried out using the PHOT function in IRAF (http://iraf.noao.edu/). The selected aperture had a radius ~3.3x the full-width at half maximum (FWHM) of the stars. The background signal was calculated from an annulus having inner radius 4x the FWHM, with a radial extent of 10 pixels.

Data from all three stars were combined to derive extinction coefficients (0.30±0.01 for *R* and 0.38±0.02 for *V*) for the night. Airmass corrections were then applied to the instrumental magnitudes in order to derive measured magnitudes. Our results, the weighted average magnitude of all frames for each object, are presented in Table 2. Established, standard star magnitudes [12-14] minus measured magnitudes are plotted for 50 frames in each filter in Figs. 3a and 3b. Mean absolute differences between the measured and established magnitudes are less than 0.02 mag. for all stars in both filters, with a maximum deviation for any single observation of 0.03 mag. The good agreement between measured and standard values indicates that POETS can achieve high photometric accuracy for bright sources.

For fainter sources, we chose to do relative photometry at Hopkins Observatory. Using POETS X-1484, we observed the core of open cluster M29 (NGC6913) on 2007 July 11 and 13. These two nights had fair transparency and seeing of ~3–4 arcsec. On each night we obtained a frame-transfer sequence (60 frames and 30 frames, respectively) through a Bessel *V* filter built into the Hopkins Observatory

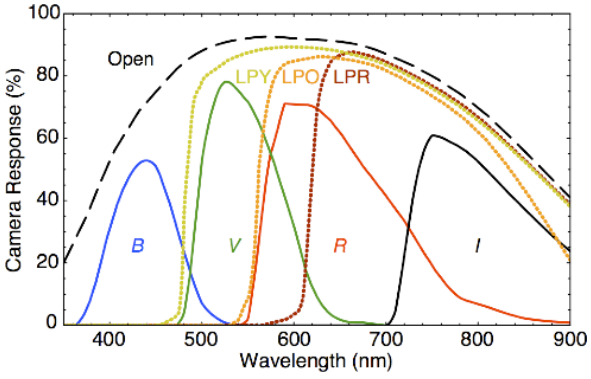

FIGURE 2. POETS camera response as a function of wavelength. The percentage response is determined by the CCD efficiency multiplied by the filter transmittance. The response is displayed for each of the system filters: solid lines represent Schüler *B*, *V*, *R*, and *I*, while dotted lines represent Baader long-pass red (610nm; LPR), orange (570 nm; LPO), and yellow (495 nm; LPY). The dashed line represents the "open" or no filter response, which is merely the quantum efficiency of the CCD.

TABLE 2. Standard stars observed to test POETS photometric accuracy.

Standard Star	*V* mag.[a]	*R* mag.[a]	Measured *V* mag.[b]	Measured *R* mag.[b]
HD161198	7.521±0.001	7.071±0.021	7.513±0.003	7.070±0.002
HD161817	6.982±0.003	6.862±0.022	6.970±0.004	6.850±0.003
HD217014	5.456±0.004	5.082±0.006	5.456±0.006	5.081±0.004

[a] Established magnitudes are from references [12-14]. [b] Errors are the average of the formal errors on individual measurements, which are calculated following reference [15].

telescope. We used conventional readout at 1 MHz, with preamp gain 4.7x and an exposure time of ~2 s. All frames were obtained at low airmass (< 1.1).

The sparsely populated cluster M29 was selected because it permits ample sky measurement around each target star, and it transits near the zenith at Hopkins. For comparison, we reference M29 observations taken at Kitt Peak National Observatory using a Harris *V* filter [16]. No attempt was made to compensate for filter bandpass differences: the Harris and Bessel filters have very similar bandpass to the Schuler *V* filter shown in Fig. 2.

Standard reduction, using sky flats taken on both nights, and aperture photometry were performed using ImageJ (http://rsb.info.nih.gov/ij/) on 25 stars spanning nearly seven magnitudes (*V* = 8.58 to 15.38). The 2-sec. cadence revealed substantial frame-to-frame variations due to scintillation, and larger aperture sizes were not feasible as they contained significant photon noise from the sky and encroached on surrounding stars. A single best frame was thus chosen for measurement from each sequence. In Fig. 3c, the ratio of measured counts to the simulated counts calculated from Massey *et. al.* [16] are displayed. If both observations were ideal, and the stars and sky unchanging, the result would be a horizontal line at value 1.0. There is instead a slight slope at brighter magnitudes. The differences between the counts are generally ≤ 5% to *V* ≈ 13.5, where the integrated star signal begins to approach the signal from the sky itself. These measurements indicate good photometric accuracy for unresolved sources from roughly half of full scale down to approximately sky brightness. The slight slope may be due to the mismatch between Bessel and Harris *V* bandpasses.

DISCUSSION

To date, our high-speed, portable systems have been extremely successfully in the task for which they were optimized: to be carried to and mounted on telescopes around

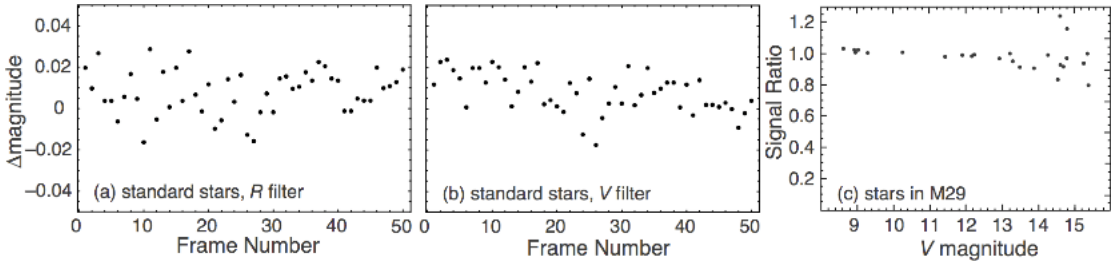

FIGURE 3. POETS photometric measurements. (a, b) The difference between measured and established [12-14] magnitudes in two different filters for three bright standard stars. Each plot contains measurements from 10 frames of HD217014 (*V* ≈ 5.46), and 20 frames each of HD161198 (*V* ≈ 7.52) and HD161817 (*V* ≈ 6.98). The measurements deviate < 0.03 mag. from the established magnitudes. (c) The ratio of measured to established counts [16] versus magnitude [16] for 25 stars in M29. The data are in good agreement at bright magnitudes (*V* < 13.5), after which point the star signal approaches the sky brightness and the relative accuracy of the POETS measurements degrades.

the world in order to observe (i) stellar occultations by planetary bodies (discussed here), (ii) a solar transit by Mercury (http://www.williams.edu/astronomy/eclipse/transits/transitofmercury.htm), (iii) solar eclipses [17, 18], and (iv) extrasolar planet transits [19]. POETS cameras achieve low read noise in conventional mode (5.6 to 6.7 e~/pixel in 1 MHz mode) and effectively reach sub-electron read noise in EM mode. Furthermore, initial measurements indicate that the systems can be used to obtain accurate photometric data.

In the future, our small-body stellar occultation work will focus on Kuiper Belt objects (KBOs). First, the diameters (and thus albedos) of many KBOs are not accurately known. Even radiometric radii that have relatively small error bars should be calibrated with stellar occultation results, since the derivation of these radii require thermal modeling assumptions concerning rotation and shape. Second, occultation observations may serendipitously result in the discovery of binaries, which are predicted to be commonplace by some binary KBO formation models [20, 21]. Finally, there is an intriguing possibility that some KBOs could retain atmospheres that would be detectable through stellar occultation observations [22]. As demonstrated by Fig. 4, the largest bodies in the outer solar system share characteristics with objects known to possess substantial atmospheres. A simple atmospheric escape model indicates that, like Pluto and Triton, volatiles should be retained on Eris, Sedna, and possibly on 136472, 136108, and Quaoar [23]. Indeed, volatiles have recently been detected on the surfaces of some of these objects: Eris, 136472, and Sedna are rich in CH_4 ice and could contain other volatiles [24-29], and N_2 ice has been detected on Eris [27] and possibly on Sedna [28, 29]. Speculation has already begun concerning the roles of sublimation, recondensation, and annual temperature variations on a possible Eris atmosphere [e.g. 27, 30].

Fabrication has commenced for a POETS to be mounted on NASA's IRTF (InfraRed Telescope Facility, 3 m) on Mauna Kea, Hawaii. We look forward to obtaining high-quality occultation observations from the IRTF, combined with our other POETS, in order to continue our study of small bodies in the outer solar system.

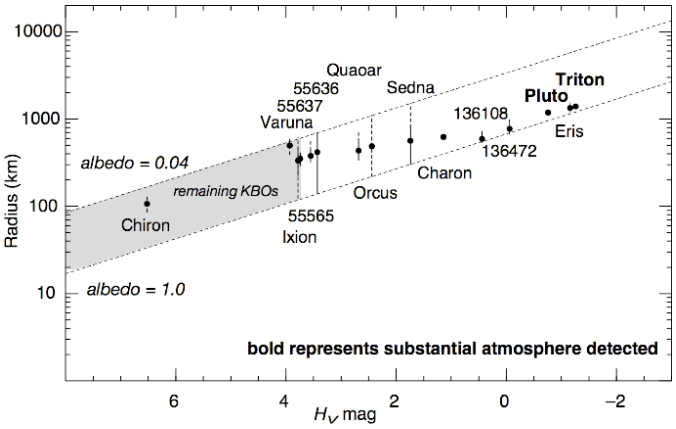

FIGURE 4. Size and magnitude as atmospheric indicators. The radii of small-body occultation targets are plotted versus absolute visual magnitude [31], and objects known to have substantial atmospheres are shown in bold font. The brightest objects are plotted individually, while the remainder of the population is represented by the shaded area. (Chiron is plotted because a stellar occultation has previously been observed [32].) The parameter space for objects having geometric albedo between 0.04 and 1.0 is demarked by dotted lines, assuming the relationship derived for asteroids [33]. Radii for Pluto, Charon, Triton, and Varuna are from [5, 9, 34, 35], respectively. All remaining objects, excluding 55637, have radii and solid error bars derived from *Spitzer Space Telescope* data [31]. Because of inherent assumptions in thermal modeling we have included additional radii error bars (dashed) to encompass non-Spitzer measurements [see 31, for references]. If no other measurements have been made, the dashed error bars include the full range of possible albedos. Figure adapted from [22].

ACKNOWLEDGMENTS

This work was supported, in part, by NASA Planetary Astronomy grants NNG 04GE48G, NNG 04GF25G, NNG 05GF75G, NNH 04ZSS001N, and NNX 07AK95G.

REFERENCES

1. S. P. Souza, B. A. Babcock, J. M. Pasachoff, A. A. S. Gulbis, J. L. Elliot, M. J. Person and J. W. Gangestad, POETS: Portable Occultation, Eclipse, and Transit System. Publ. Astron. Soc. Pacific 118, 1550-1557 (2006).
2. S. W. McDonald and J. L. Elliot, Erratum: "Pluto-Charon stellar occultation candidates: 2000-2009" [Astron. J. 119, 1999 (2000)]. Astron. J. 120, 1599-1602 (2000).
3. N. Zacharias, S. E. Urban, M. I. Zacharias, G. L. Wycoff, D. M. Hall, D. G. Monet and T. J. Rafferty, The second US Naval Observatory CCD Astrograph Catalog (UCAC2). Astron. J. 127, 3043-3059 (2004).
4. A. R. Walker, An occultation by Charon. Mon. Not. Roy. Astron. Soc. 192, 47p-50p (1980).
5. J. L. Elliot, M. J. Person, A. A. S. Gulbis, S. P. Souza, E. R. Adams, B. A. Babcock, J. W. Gangestad, A. E. Jaskot, E. A. Kramer, J. M. Pasachoff, R. E. Pike, C. A. Zuluaga, A. S. Bosh, S. W. Dieters, P. J. Francis, A. B. Giles, J. G. Greenhill, B. Lade, R. Lucas and R. D. J., Changes in Pluto's atmosphere: 1988-2006. Astron. J. 134, 1-13 (2007).
6. M. J. Person, J. L. Elliot, A. A. S. Gulbis, C. A. Zuluaga, B. A. Babcock, A. J. McKay, J. M. Pasachoff, S. P. Souza, W. B. Hubbard, C. A. Kulesa, D. W. McCarthy, S. D. Kern, S. E. Levine, A. S. Bosh, E. V. Ryan, W. H. Ryan, A. Meyer and J. Wolf, Waves in Pluto's Upper Atmosphere. Astron. J., in preparation (2007).
7. A. A. S. Gulbis, J. L. Elliot, M. J. Person, E. R. Adams, B. A. Babcock, M. Emilio, J. W. Gangestad, S. D. Kern, E. A. Kramer, D. J. Osip, J. M. Pasachoff, S. P. Souza and T. Tuvikene, Charon's radius and atmospheric constraints from observations of a stellar occultation. Nature 439, 48-51 (2006).
8. M. J. Person, J. L. Elliot, A. A. S. Gulbis, C. A. Zuluaga, B. A. Babcock, A. J. McKay, J. M. Pasachoff, S. P. Souza, W. B. Hubbard, C. A. Kulesa, D. W. McCarthy, S. D. Kern, S. E. Levine, A. S. Bosh, E. V. Ryan, W. H. Ryan, A. Meyer and J. Wolf, (134340) Pluto. International Astronomical Union Circulars No. 8825 (2007).
9. M. J. Person, J. L. Elliot, A. A. S. Gulbis, J. M. Pasachoff, B. A. Babcock, S. P. Souza and J. W. Gangestad, Charon's radius and density from the combined data sets of the 2005 July 11 occultation. Astron. J. 132, 1575-1580 (2006).
10. D. McCarthy, C. Kulesa, W. Hubbard, S. D. Kern, M. J. Person, J. L. Elliot and A. A. S. Gulbis, Occultation Measurement of Gravity Wave Breaking in Pluto's High Atmosphere. Science, submitted (2007).
11. D. W. McCarthy, C. A. Kulesa, W. B. Hubbard, S. D. Kern, M. J. Person, J. L. Elliot and A. A. S. Gulbis, (134340) Pluto. International Astronomical Union Circulars No. 8825 (2007).
12. A. U. Landolt, UBVRI Photometry of Stars Useful for Checking Equipment Orientation Stability. Astron. J. 88, 853-866 (1983).
13. F. Morale, G. Micela, F. Favata and S. Sciortino, Stromgren Four-Color Photometry of X-ray Active Late-Type Stars: Evidence for Activity Induced Deficiency in the m1 Index. Astronomy and Astrophysics, Supplement Series 119, 403-412 (1996).
14. B. J. Taylor, Transformation Equations and Other Aids for VRI Photometry. Astrophysical Journal Supplement Series 60, 577-599 (1986).
15. A. A. S. Gulbis, J. L. Elliot and J. F. Kane, The color of the Kuiper belt core. Icarus 183, 168-178 (2006).
16. P. Massey, K. E. Johnson and K. DeGioia-Eastwood, The Initial Mass Function and Massive Star Evolution in the OB Associations of the Northern Milky Way Galaxy. Astrophys. J. 454, 151-171 (1995).
17. J. M. Pasachoff and M. A. Bruck, High-Spectral-Resolution Observations of the Solar Chromosphere and Corona. Bull. Amer. Astron. Soc. 39, 224 (2007).

18. J. M. Pasachoff, B. A. Babcock, S. P. Souza, M. A. Bruck, P. W. Hess, S. B. Kimmel, J. S. Levitt, A. S. Steele, A. E. Tsykalova, D. M. Rust, M. W. Noble, R. A. Wittenmyer, J. Kern, R. L. Hawkins, J. H. Seiradakis, A. Voulgaris, G. Pistikoudis, J. Nestoras and M. Demianski, Coronal Observations at the 29 March 2006 Total Solar Eclipse. Bull. Amer. Astron. Soc. 38, 216 (2006).
19. E. R. Adams, M. Lopez-Morales, J. L. Elliot, S. Seager and D. J. Osip, A Study of Transiting Extrasolar Planets Using Magellan. Bull. Amer. Astron. Soc. 38, 494 (2006).
20. P. Goldreich, Y. Lithwick and R. Sari, Formation of Kuiper-belt binaries by dynamical friction and three-body encounters. Nature 420, 643-646 (2002).
21. S. A. Astakhov, E. Lee, A. and D. Farrelly, Formation of Kuiper-belt binaries through multiple chaotic scattering encounters with low-mass intruders. Mon. Not. Roy. Astron. Soc. 360, 401-415 (2005).
22. J. L. Elliot and S. D. Kern, Pluto's atmosphere and a targeted-occultation search for other bound KBO atmospheres. Earth, Moon, and Planets 92, 375-393 (2003).
23. E. L. Schaller and M. Brown, Volatile Loss and Retention on Kuiper Belt Objects. Astrophys. J. Lett. 659, L61 (2007).
24. M. E. Brown, K. M. Barkume, G. A. Blake, E. L. Schaller, D. L. Rabinowitz, H. G. Roe and C. A. Trujillo, Methane and ethane on the bright Kuiper Belt object 2005 FY9. Astron. J. 133, 284-289 (2007).
25. M. E. Brown, C. A. Trujillo and D. L. Rabinowitz, Discovery of a planetary-sized object in the scattered Kuiper belt. Astrophys. J. Lett. 635, L97-L100 (2005).
26. J. Licandro, N. Pinilla-Alonso, M. Pedani, E. Oliva, G. P. Tozzi and W. Grundy, The methane ice rich surface of large TNO 2005 FY9: a Pluto-twin in the trans-neptunian belt? Astron. & Astrophys. 445, L35-L38 (2006).
27. J. Licandro, W. Grundy, N. Pinilla-Alonso and P. Leisy, Visible spectroscopy of 2003UB313: Evidence for N2 ice on the surface of the largest TNO? Astronomy and Astophysics 458, L5-L8 (2006).
28. M. A. Barucci, D. Cruikshank, E. Dotto, F. Merlin, F. Poulet, C. Dalle Ore, S. Fornasier and C. De Bergh, Is Sedna another Triton? Astronomy and Astophysics 439, L1-L4 (2005).
29. J. P. Emery, C. M. Dalle Ore, D. P. Cruikshank, Y. R. Fernandez, D. E. Trilling and J. A. Stansberry, Ices on (90377) Sedna: Confirmation and compositional constraints. Astron. & Astrophys. 466, 395-398 (2007).
30. M. E. Brown, E. L. Schaller, H. G. Roe, D. L. Rabinowitz and C. A. Trujillo, Direct measurement of the size of 2003 UB313 from the Hubble Space Telescope. Astrophys. J. Lett. 643, L61-L63 (2006).
31. J. A. Stansberry, W. Grundy, M. Brown, D. Cruikshank, J. Spencer, D. E. Trilling and J. L. Margot, Physical Properties of Kuiper Belt and Centaur Objects: Constraints from Spitzer Space Telescope, in Kuiper Belt, M. A. Barucci, H. Boehnhardt, D. Cruikshank and A. Morbidelli, (Eds), U. Arizona Press, Tucson, 2007.
32. S. J. Bus, M. W. Buie, D. G. Schleicher, W. B. Hubbard, R. L. Marcialis, R. Hill, L. H. Wasserman, J. R. Spencer, R. L. Millis, O. G. Franz, A. S. Bosh, E. W. Dunham, C. H. Ford, J. W. Young, J. L. Elliot, R. Meserole, C. B. Olkin, S. W. McDonald, J. A. Foust, L. M. Sopata and R. M. Bandyopadhyay, Stellar occultation by 2060 Chiron. Icarus 123, 478-490 (1996).
33. E. Bowell, B. Hapke, D. Domingue, K. Lumme, J. Peltoniemi and A. W. Harris, Application of photometric models to asteroids, in Asteroids II, R. P. Binzel, T. Gehrels and M. S. Matthews, (Eds), Tucson, 1989, pp. 524-556.
34. P. C. Thomas, The Shape of Triton from Limb Profiles. Icarus 148, 587-588 (2000).
35. D. Jewitt, H. Aussel and A. Evans, The size and albedo of the Kuiper Belt Object (20000) Varuna. Nature 411, 446-447 (2001).